Paddy and Water Environment
https://doi.org/10.1007/s10333-024-00968-8

ARTICLE

Modeling the impacts of natural and anthropogenic processes on the hydrologic components in Kordan watershed, Iran

Majid Altafi Dadgar[1] · **Hossein Mohammadzadeh**[1,2]

Received: 9 December 2022 / Revised: 6 December 2023 / Accepted: 21 December 2023

Abstract
The objective of this study was to investigate impacts of climate disturbance and watershed management operations on hydrologic functioning of the Kordan watershed in Iran. Soil and water assessment tool was used and evaluated for an 18-year monthly stream discharge. Statistical and graphical analysis of the calibrated and validated model presented appropriate fit to the measured data (NSE and R^2 were more than 0.80), allowing reproduction of the historic hydrological conditions of the watershed for future analysis. A 12-month timeframe was achieved from correlation between standardized precipitation index and standardized runoff index to quantify drought characteristics and define drought disturbance scenarios. Replacing normal periods in terms of precipitation amount with extreme and severe periods up to 40% resulted in declining monthly flow out by 24% and 21%, respectively. Pasture restoring scenarios resulted in a significant decline in amount of surface runoff. Replacing 50% of poor rangeland areas with moderate rangeland caused monthly amount runoff to decline by 16%. The percentage of runoff decline raised up to 44% by replacing moderate rangeland thoroughly. Furthermore, land-use scenarios increased amount of subsurface flow considerably. Impacts of constructing hydraulic structures were assessed in each sub-basin separately. Results showed decline in yearly surface runoff varied from 50 to 97%, depending on the volume of structures and sub-basin characteristics. The findings would be beneficial to decision makers which contribute to better understanding of natural and man-made activities on hydro-power potential of watersheds.

Keywords SWAT model · Land-use changes · Climate disturbance · Hydraulic structures

Introduction

The quantity of water provided by a watershed is an indicator suggesting the amount and intensity of rainfall as well as watershed management operations. To investigate water production potential of a watershed, there is necessity of analyzing different factors, affecting hydrological processes (Ghoraba 2015). These factors can be generally grouped into two categories, including natural factors and anthropogenic activities (Wu et al. 2019). One of the main natural factors is climate disturbance which can pose a critical threat to stability of water resources. To assess future water supply resources, water managers and decision makers often plan on assumptions that precipitation does not change over time (Mukheibir 2007). However, the statistical distribution of climate patterns is changing and its impacts should be more addressed. On the other hand, anthropogenic activities such as changing land-use and building small dams definitely alter the hydrological functioning of a watershed (Tamm et al. 2018). Obviously, analysis of these factors requires modeling tools that can simulate complex hydrological processes. Such models provide a variety of options to decipher the effects of natural and anthropogenic factors in a watershed (Francesconi et al. 2016). It also prepares conceptual frameworks for making decisions on watershed management operations (Ndulue et al. 2018). Among hydrological models soil and water assessment tool (SWAT), a physically based and semi-distributed model (Arnold et al. 1998) has been applied in many studies to simulate the effects of land-use and climate changes (Gathenya et al. 2011; Jung et al. 2013;

✉ Majid Altafi Dadgar
Dadgarmajid77@yahoo.com

[1] Groundwater and Geothermal Research Center (GRC), Water and Environment Research Institute, Ferdowsi University of Mashhad, Mashhad, Iran

[2] Groundwater and Geothermal Research Center, Water and Environment Research Institute, Department of Geology, Faculty of Science, Ferdowsi University of Mashhad, Mashhad, Iran

Published online: 07 February 2024

Qasim et al. 2013; Salmoral et al. 2015; Tamm et al. 2018; Wang et al. 2018; Osei et al. 2019; Kim et al. 2020; Lin et al. 2022), watershed management (Jain et al. 2010; Fan and Shibata 2014; Rodrigues et al. 2014; Ghoraba 2015) and impacts of hydrological structures (Piman et al. 2013; Angela et al. 2015; Li et al. 2016; Norman and Niraula 2016; Shi et al. 2019) at watershed and regional scales. Most of the above-mentioned studies have mainly focused on assessing the impacts of human- and natural-induced activities on changes in surface water components, including runoff, evapotranspiration, surficial soil–water storage, water quantity and quality. However, the impacts on subsurface flow and the whole productivity of water in watersheds have not been received sufficient attention. Furthermore, how hydrological processes of different sub-basins respond to human activities while receiving the same amount of precipitation has not been clearly assessed. Moreover, each watershed is unique in physical and geometric characteristics, water productivity, land cover and climatological conditions. In other words, results of watershed management operations vary from place to place and may not be generalized. Therefore, these cases underline the need for new research to decipher the hydrological functioning and water productivity of watersheds in response to any induced changes. This study aimed at analyzing the impacts of anthropogenic- and climate-induced disturbances on the hydrological functioning of a semiarid watershed in Iran.

Study area

Kordan watershed is located in the upper reaches of the Karaj river, in Alborz province of Iran (50°50′–51°06E, 35°52′–36°06′), extending over an area of 357 Km^2 (Fig. 1). The area has a semiarid climate, and it receives 398 mm of precipitation annually. The area's yearly temperature is 13 °C with an average annual evaporation of 1286 mm. Rainfall events take place from December to May (more than 80% of the events), but the storms mainly occur in May and June, causing flash floods to happen. The elevation of the watershed ranges from 1410 to 4108 m above sea level, with an average slope of 44%. From geological point of view, the watershed is dominantly covered by andesite, tuff, sandstone and shale units and partially by alluvial deposits. Poor vegetation covers alongside weathered and fractured geological units have made the occurrence of flash floods more likely, resulting in sediment yield of approximately 2800 tons annually (Sarmadian et al. 2010). Since 2016, some watershed management operations have been applied to the study area in order to alleviate flood damage. The operations include physical

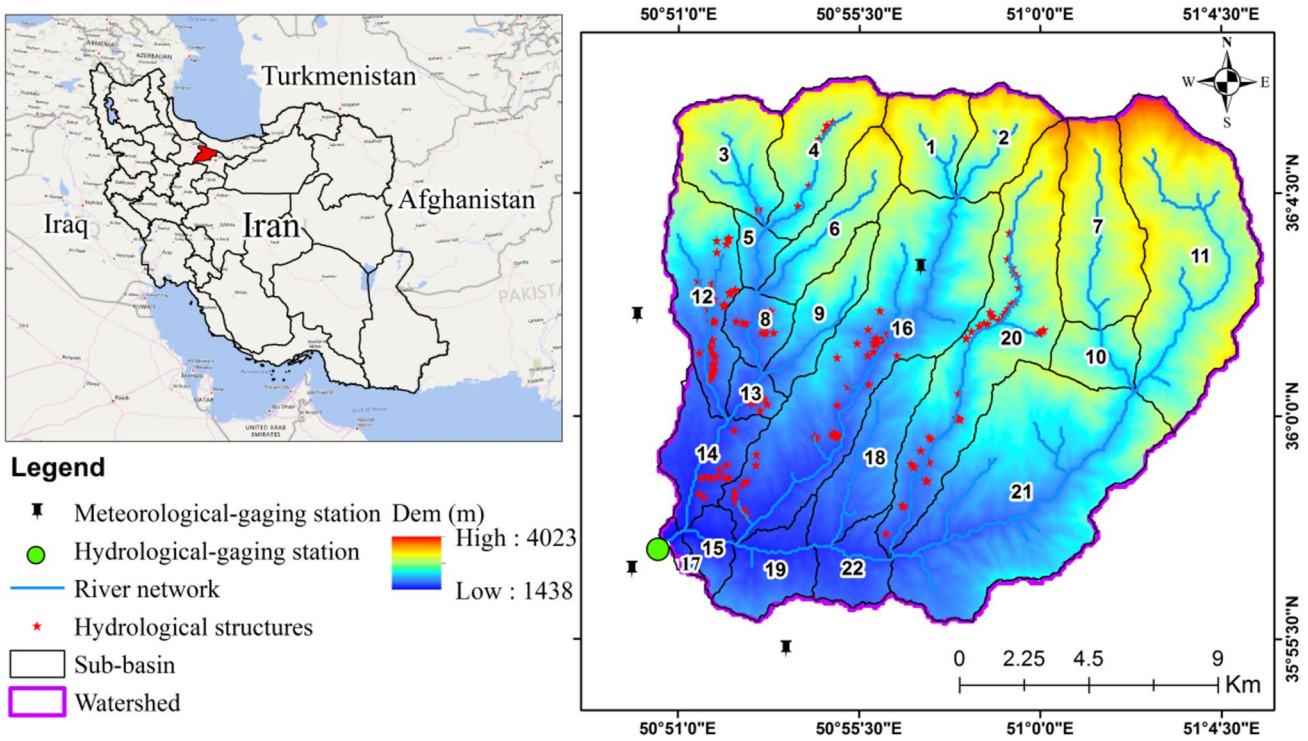

Fig. 1 Location map of the study area accompanied by the representation of sub-basins, meteorological- and hydrological-gaging stations and hydraulic structures

and biological activities such as constructing small dams, gabions, check dams and pasture restoration (Sazeh-Ab-Shafagh Co. 2016).

Materials and methods

SWAT model and setup

Soil and water assessment tool (SWAT) is a watershed-scale, semi-distributed and physical-based model which has been developed in order to simulate hydrological processes. SWAT enables it to simulate watershed systems, forecasting the impact of land management operations on water, sediment and agricultural chemical yields (Arnold et al. 1998). It simulates hydrologic cycle based on the water balance equation (Eq. 1):

$$SW_t = SW_0 + \sum_{i=1}^{n} (R_{day} - Q_{surf} - E_a - W_{seep} - Q_{gw}) \quad (1)$$

where SW_t is the final soil moisture, SW_0 is the initial soil moisture, R_{day} is the amount of precipitation, Q_{surf} is the amount of surface runoff, E_a is the amount of evapotranspiration, W_{seep} is the amount of percolation and Q_{gw} stands for the amount of base flow, all in mm H_2O, and n is the number of days.

The model is flexible in watershed delineation by placing the outlet point at anywhere of the main reach and provides the facilities to compare the results of simulated discharge with hydrological observed data. The SWAT workflow can include delineation of watershed, dividing it into sub-basins, hydrological response unit (HRU), sensitivity analysis, model calibration and verification. In this study, 22 sub-basins were delineated and linked to the same number of HRUs based on the unique combination of land-use, soil and slope layers (Fig. 1). The Hargreaves method was used to estimate potential evapotranspiration (Hargreaves and Samani 1982), and the soil conservation service curve number method (SCS) was used to estimate the amount of runoff.

Table 1 presents data types and sources used to set up the model. To delineate the watershed, digital elevation map of the area (DEM) with a pixel size of 30 m was used. This map was obtained from the designated online source (https://earthexplorer.usgs.gov/). The slope map was extracted from DEM and classified into five categories, including 0–10, 10–20, 20–40, 40–60 and > 60% (see Fig. 2a). The soil layer was obtained from the 1:250,000 map of the Kordan land capability, provided by Forests, Range and Watershed Management Organization of Alborz province (Sazeh-Ab-Shafagh Co., 2016; Sabz-AndishPayesh Co., 2018). Major soil types included clay-sand, loamy-sand, loam, clay-loam, sand, sandy-clay, loamy-clay-sand, alluvial soil and lithic soil. Monthly discharge data of the Kordan hydrological-gaging station were used for simulation period from 1998 to 2016. Furthermore, daily climate measurements were obtained from five meteorological-gaging stations (Fig. 1) from January 1998 to January 2016. Meteorological data also were used to conduct drought analysis. Information on hydraulic structure characteristics was obtained from the archived data by Forests, Range and Watershed Management Organization (Sazeh-Ab-Shafagh Co., 2016).

For providing the land-use map, an effort was made to derive it from Landsat 8 OLI_TIRS images in 2016. These images retrieved from open data sources websites on earth observations (www.gscloud.cn). The images were analyzed by supervised classification method in analysis tool package of ArcGIS 10.8 (ESRI), and the accuracy of the extracted layer was examined by visual check points and field investigations. The land-use map was classified into six classes (Anderson et al. 1976), including mixed urban and built-up land (URMD), orchard of fruit tress (ORCD), poor rangeland (RANGB), moderate rangeland (RANGE), stream and ponds (WATR) and barren land (BARR). The extracted map was used as the basic land-use map for simulation period (Fig. 2b).

Model calibration

Calibration of the model parameters and verification processes were performed using SUFI-2 algorithm (Sequential Uncertainty Fitting Procedure Version 2) in SWAT-CUP program (Abbaspour 2011). Monthly discharge data from Kordan gaging station were used to calibrate and validate the model. Calibration was performed with the observed data from 2002 to 2012, and for validation measured data from

Table 1 Data types used to set up SWAT model of the study area

Data type	Data source	Spatial/temporal resolution
DEM	https://earthexplorer.usgs.gov/	Grid cell 30 m × 30 m
Soil map	Forests, Range and Watershed Management Organization of Alborz province	1: 250,000
Land-use	www.gscloud.cn (Landsat 8 OLI_TIRS images)	Grid cell 30 m × 30 m
Climate	http://alborzmet.ir/?lang=en-us	Daily
River discharge	https://www.albrw.ir/?l=EN	Monthly

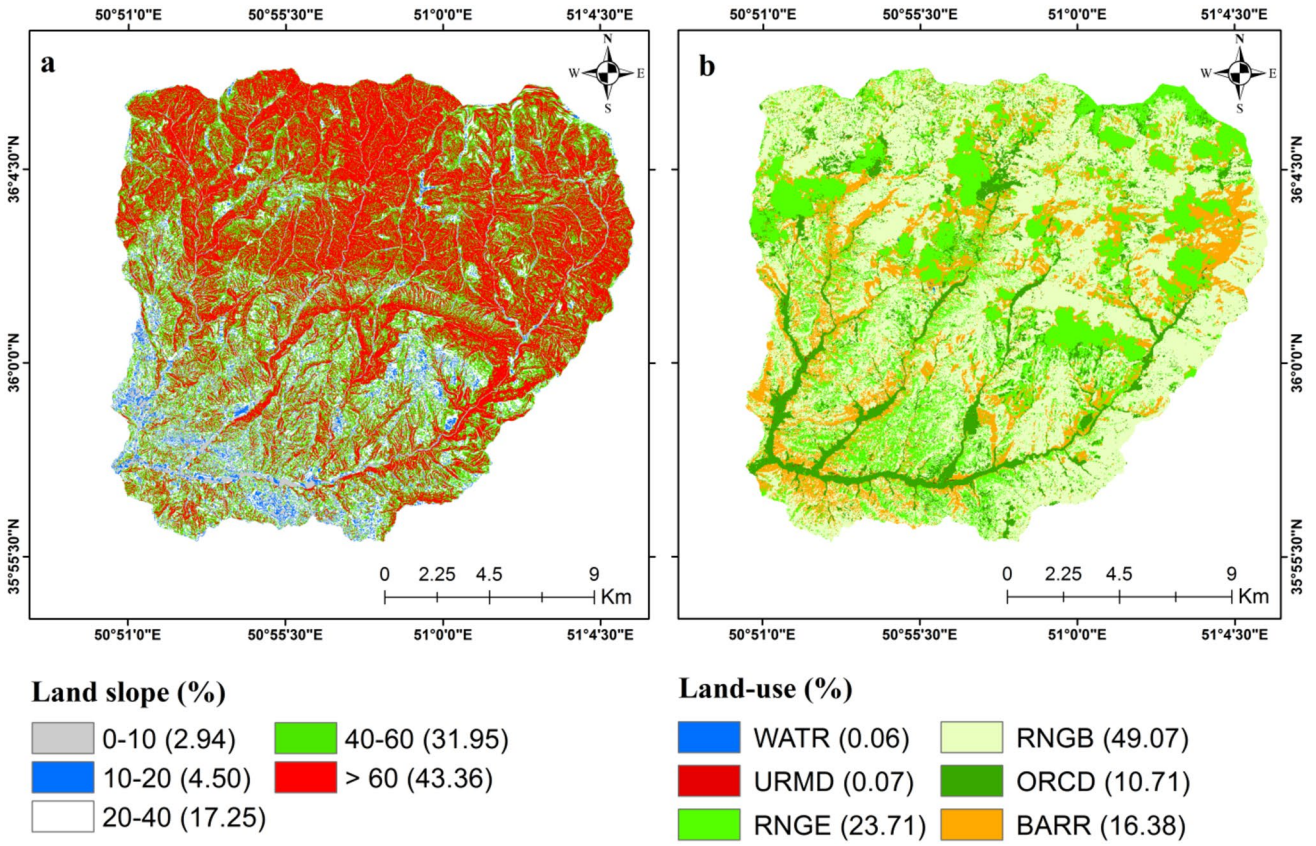

Fig. 2 Spatial pattern of the classified land slope map (**a**) and land-use map of the study area (**b**)

2012 to 2016 were used. Moreover, a four-year time step (1988–2002) was set as a warm-up period. To assess the performance of the model results, goodness-of-fit analysis was conducted using statistics of comparing model results and observed data through coefficient of determination (R^2), Nash–Sutcliffe efficiency (NSE, Nash and Sutcliffe (1970)), percent bias (PBIAS, Gupta et al. (1998)) and standardized percent bias (RSR, Moriasi et al. (2007)).

Climate scenario

One of the main factors to evaluate climate changes is to analyze how temporal pattern of the precipitation has been changing over a certain period. In other words, climate changes are mainly reflected in the amount of precipitation (Thornton et al. 2006; Bobadoye et al. 2016; Gao et al. 2020). Therefore, the standardized precipitation index (SPI) was used to assess drought periods and temporal variability of rainfall amounts (McKee et al. 1993). The SPI is an indicator which represents the probability of rainfall occurrence in a certain time scale (Eq. (2)).

$$\mathrm{SPI}_{ij} = \frac{P_{ij} - \bar{P}_{ij}}{\delta_{ij}} \tag{2}$$

where SPI_{ij} is the score deviation from the mean in units of the standard deviation during timeframe i for year j, P_{ij} is the precipitation value during timeframe i for year j, $\bar{P}_{ij}$ is the mean during timeframe i over n years, and σ_{ij} is the standard deviation during timeframe i for year j. The drought classification based on the SPI is shown in Table 2. It was necessary to reveal by which timeframe of the SPI analysis, propagation of drought could be presented better (Porhemmat and Altafi Dadgar 2023). Hence, standardized runoff

Table 2 Drought categories based on the SPI values (Adapted from McKee et al. (1993))

SPI values	Drought category
≥ 0	Normal
0 to − 0.99	Mild
− 1 to − 1.49	Moderate
− 1.50 to − 1.99	Severe
≤ − 2.00	Extreme

index (SRI) was calculated and correlated with the SPI and finally the best timeframe was determined based on the maximum correlation coefficient. The SRI utilizes the same concepts as the SPI (Shukla and Wood 2008). The upper limit of precipitation amount and duration of drought were quantified for each drought classification. Climate scenarios were defined by replacing the amount of precipitation in normal years with the amount precipitation of in extreme and severe years. Two climate scenarios (S1Cs) were defined: S1C1 and S1C2. In S1C1, duration of normal drought was reduced up to 40% and replaced by extreme drought characteristics. In S1C2, similar assumption was taken except for replacing it by severe drought characteristics. It should be mentioned that a baseline was needed to compare the results of scenarios. Thus, the outputs of the model during the simulation period were taken as the baseline to be compared with the impacts of the scenarios.

Land-use scenarios

Land-use change is one of the factors which controls discharge and sediment yield in a watershed. Pasture restoration has been started in the Kordan watershed since 2016 and implemented the parts where covered by poor range land (RANGB). To investigate the effects of these operations, two land-use scenarios (S2L) were defined. In the first scenario (S2L1), 50% of the area covered by poor rangeland (RANGB) was replaced by the moderate rangeland (RANGE). For the second one (S2L2), it was assumed that the RANGB would replace by RANGE thoroughly.

Hydraulic structure scenario:

The hydraulic structure scenario (S3H) takes the assumptions that the climate and land-use conditions are the same as the inputs applied for the simulation period except for the operation time of these structures. The model needed running for a longer period of time to present the effects of constructing the hydraulic structures over the watershed. Hence, it was assumed the operation of these structures had been started at the beginning of the simulation period. Hydraulic structures include check dams, gabions and small dams with the total storage volume of 4×10^4 m^3. These structures have been operated in eight sub-basins, including sub-basin 3, 4, 8, 12, 13, 14, 16 and 20. Information of the hydraulic structures is listed in Table 3. Due to the semi-distributive characteristic of the SWAT model, volumes of the hydrological structures were summed up for each HRU and were defined using pond (.pnd) package for the model. All the structures were constructed in 2016 and have been in regular operation.

Table 3 Hydraulic structure characteristics in Kordan watershed

Total volume (m^3)	Contributing area (ha)	Number of structure	Sub-basin number
2730	1388.75	2	3
4020	1563.69	12	4
2030	554.89	10	8
11,520	1643.02	40	12
1530	338.46	8	13
1710	1109.66	11	14
8100	4901.15	54	16
11,820	3639.29	47	20

Results and discussion

Model results

The initial run of the model was based on the default parameter values which needed calibrating to achieve the best simulation of monthly discharge data. A global sensitivity analysis method was conducted to test the sensitivity of parameters. Result showed that only 19 parameters were sensitive to the water discharge (Table 4). The most sensitive parameter was initial SCS runoff curve number (CN2), and the second one was base flow alpha factor (ALPHA_BF) which correspond to the surface and groundwater processes, respectively (Table 4).

To analyze the performance of the model results, monthly discharge of the Kordan station was compared to the model output. Figure 3 shows the best simulation of the model comparing to the observed data. Except for underestimated discharge flow in April 2007, there was consistency between seasonal fluctuations of observed and simulated discharges. A continuous wet period was recorded from 2003 to 2008 which resulted in an extreme discharge in April 2007. However, statistical parameters for calibration period proved that the performance of model was satisfactory. For this period, the values of R^2, NSE, PBIAS and RSR were 0.87, 0.81, 0.52 and 0.41, respectively. Moreover, results of the validation period showed a good correspondence between simulated and measured stream discharge data. For validation step, coefficient of determination and Nash–Sutcliffe were both larger than 0.80 and the errors were within an acceptable range, reflecting in PBIAS and RSR 0.48 and 0.55, respectively.

The main components of water budget in a watershed are precipitation, evapotranspiration, surface runoff, lateral flow, base flow and percolation. Figure 4 shows monthly

Table 4 List of the model parameters that were calibrated and their final fitted values

Parameters	Description	Fitted value	Min value	Max value
† R_CN2.mgt	Initial SCS runoff curve number for moisture condition II	− 0.03	− 0.71	0.10
V_ALPHA_BF.gw	Base flow alpha factor	0.07	0.00	1.00
V_GW_DELAY.gw	Groundwater delay time	31.89	0.63	250.70
V_GWQMIN.gw	Threshold depth of water in the shallow aquifer (for return flow)	2.41	0.00	10.00
R_SOL_AWC.sol	Available water capacity of the soil layer	− 0.06	− 0.50	0.50
R_SOL_BD.sol	Soli bulk density	− 0.25	− 0.26	− 0.25
V_CH_K2.rte	Effective hydraulic conductivity in the main alluvium channel	77.52	2.34	80.24
V_CH_N2.rte	Manning's "n" coefficient main channel	0.49	0.49	0.51
R_SOL_K.sol	Saturated hydraulic conductivity	− 0.28	− 0.56	− 0.14
V_ESCO.hru	Soil evaporation compensation factor	1.04	1.02	1.05
V_GW_REVAP.gw	Groundwater re-evaporation coefficient	0.14	0.14	0.16
R_OV_N.hru	Manning's "n" coefficient for overland flow	− 0.03	− 0.08	− 0.03
V_SMTMP.bsn	Snow melt base temperature	13.73	8.36	15.98
V_SFTMP.bsn	Snow fall temperature	6.23	3.46	9.99
R_TIMP.bsn	Snow melt temperature lag factor	0.39	0.23	0.51
V_SMFMX.bsn	Melt factor for snow on June 21	13.82	7.27	14.43
V_SMFMN.bsn	Melt factor for snow on December 21	5.57	0.98	5.69
V_CANMX.hru	Maximum canopy storage	− 15.13	− 31.36	56.36
V_GW_SPYLD	Specific yield of the shallow aquifer	0.12	0.00	0.20

† v_: refers to the substitution of a parameter by a value from the given range, r_: refers to a relative change in the parameter where the current value is multiplied by 1 plus a factor in the given range

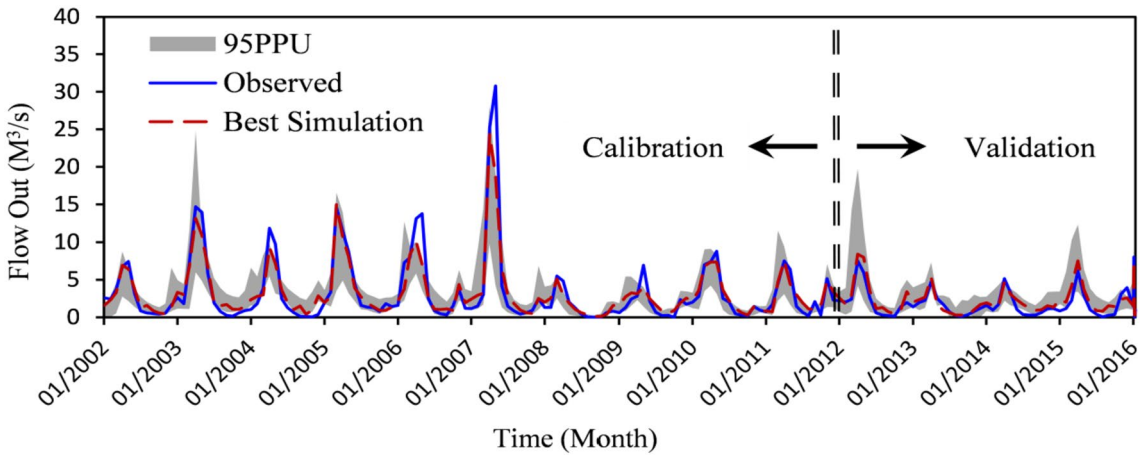

Fig. 3 Monthly time series of observed and simulated discharges at the outlet of the Kordan watershed for calibration and validation periods

average of these components during the simulation period. Evapotranspiration was one of the main contributors to water losses (~ 31%) in the watershed. The proportion of surface runoff and base flow to precipitation was ~ 26.5% and ~ 36.5%, respectively. Moreover, percentage of precipitation which infiltrated into the soil profile and contributed to percolation was ~ 18%.

Drought indices

Table 5 summarizes results of the correlation between the SPI and the SRI indices for different timeframes, including 1, 3, 6 and 12 months. The correlation coefficient was stronger when accumulation (timeframe) period increased.

The maximum correlation coefficient ($r = 0.73$) was reached when indices were both accumulated over 12 months (i.e., SPI-12 and SRI-12). The minimum correlation

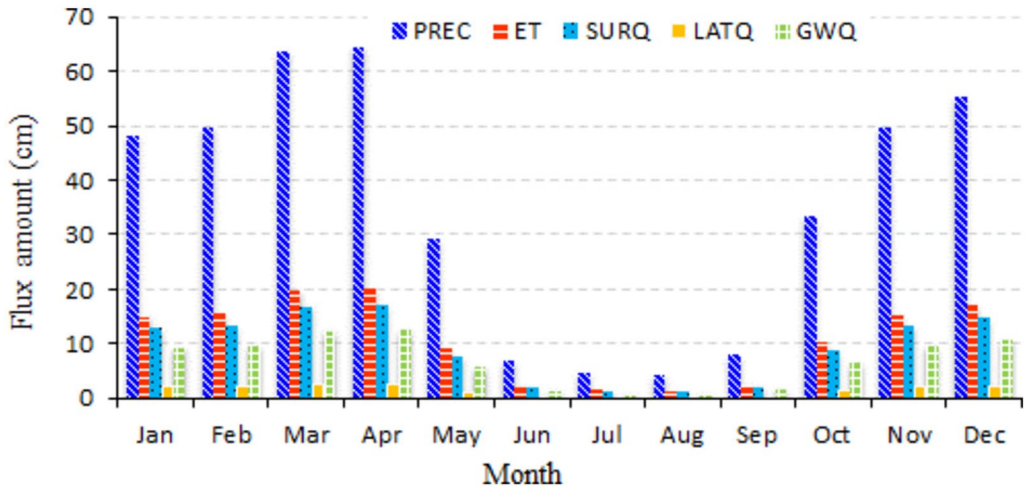

Fig.4 Monthly average water balance components during the simulation period (PREC: precipitation, ET: evapotranspiration, SURQ: surface runoff, LATQ: lateral flow, GWQ: Base flow)

Table 5 Correlation coefficient between the SPI and the SRI

	SPI-1	SPI-3	SPI-6	SPI-12
SRI-1	0.10			
SRI-3	0.08	0.40		
SRI-6	0.03	0.30	0.61	
SRI-12	0.06	0.26	0.49	**0.73**

coefficient achieved for SPI-1 and SRI-1 to 12. This might be due to the fact that the SRI is based on both surface and base flow and is affected by the time lag in contributing base flow to stream discharge.

Figure 5 shows the values of the SPI for accumulation period of 12 months in which the percentile (frequency) of extreme and severe droughts had the same value (11%). There were eight normal years, four mild years and the same number of moderate, severe and extreme drought years (2 years) during simulation period.

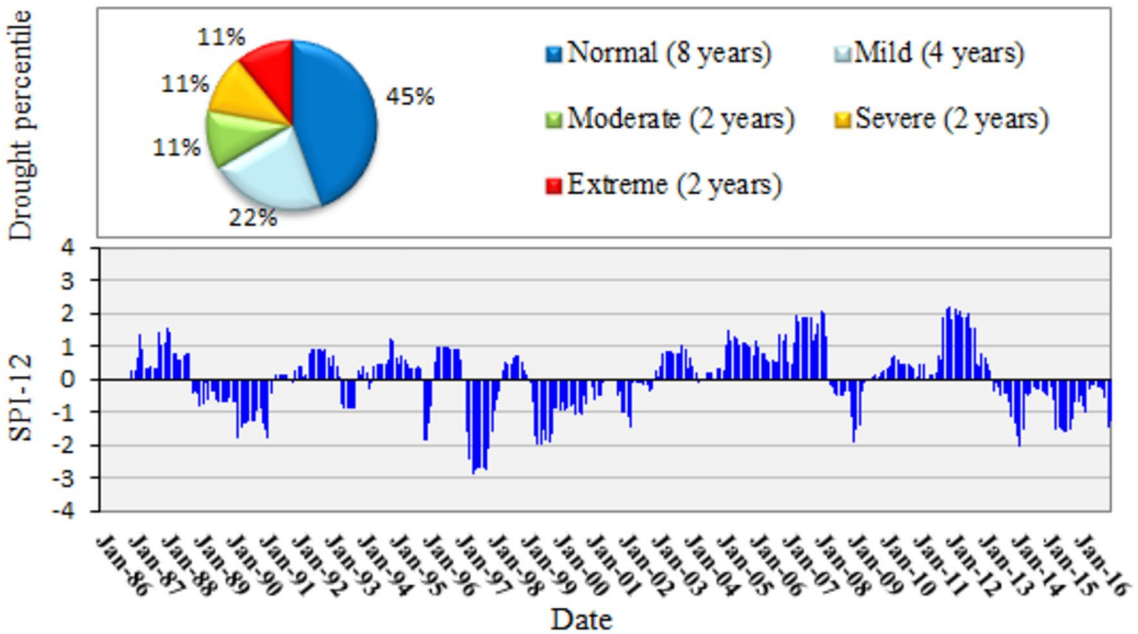

Fig. 5 The SPI values for 12-month accumulation timeframe along with the percentile of drought categories

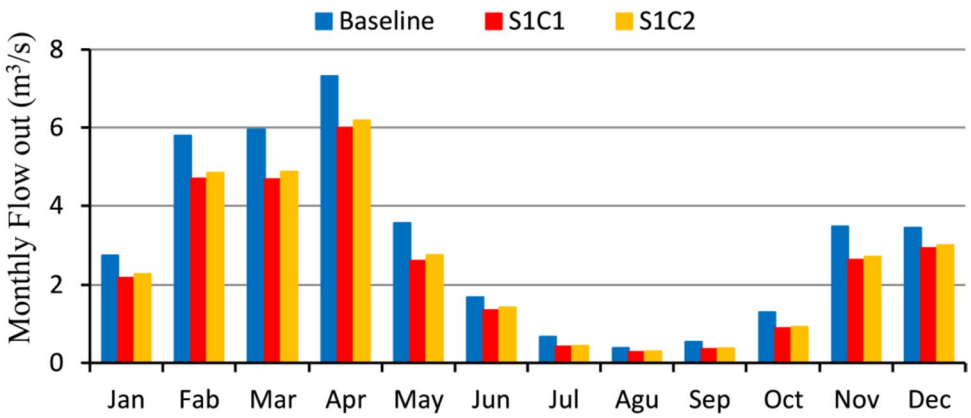

Fig. 6 The effects of the extreme drought (S1C1) and severe drought (S1C2) scenarios on monthly stream flow compared to the baseline

Climate scenarios

The impact of drought scenarios on the stream flow comparing to the baseline, i.e., amount of monthly average stream flow during the simulation period, is presented in Fig. 6. Results showed that the amount of the stream flow significantly decreased in wet months. For example, in April, monthly flow out declined by 18% and 15% for S1C1 and S1C2, respectively. It was not surprising that the amount of changes in flow out was negligible in dry months, since base flow was the main contributor to the stream flow. Precipitation deficit had significant effects on surface runoff in wet months and declined base flow contribution to streams in dry months. These findings are in consistent with the results of the previous study by Karlsson et al. (2016). Moreover, difference between effects of extreme and severe drought (intensity of drought) on changes in stream flow became

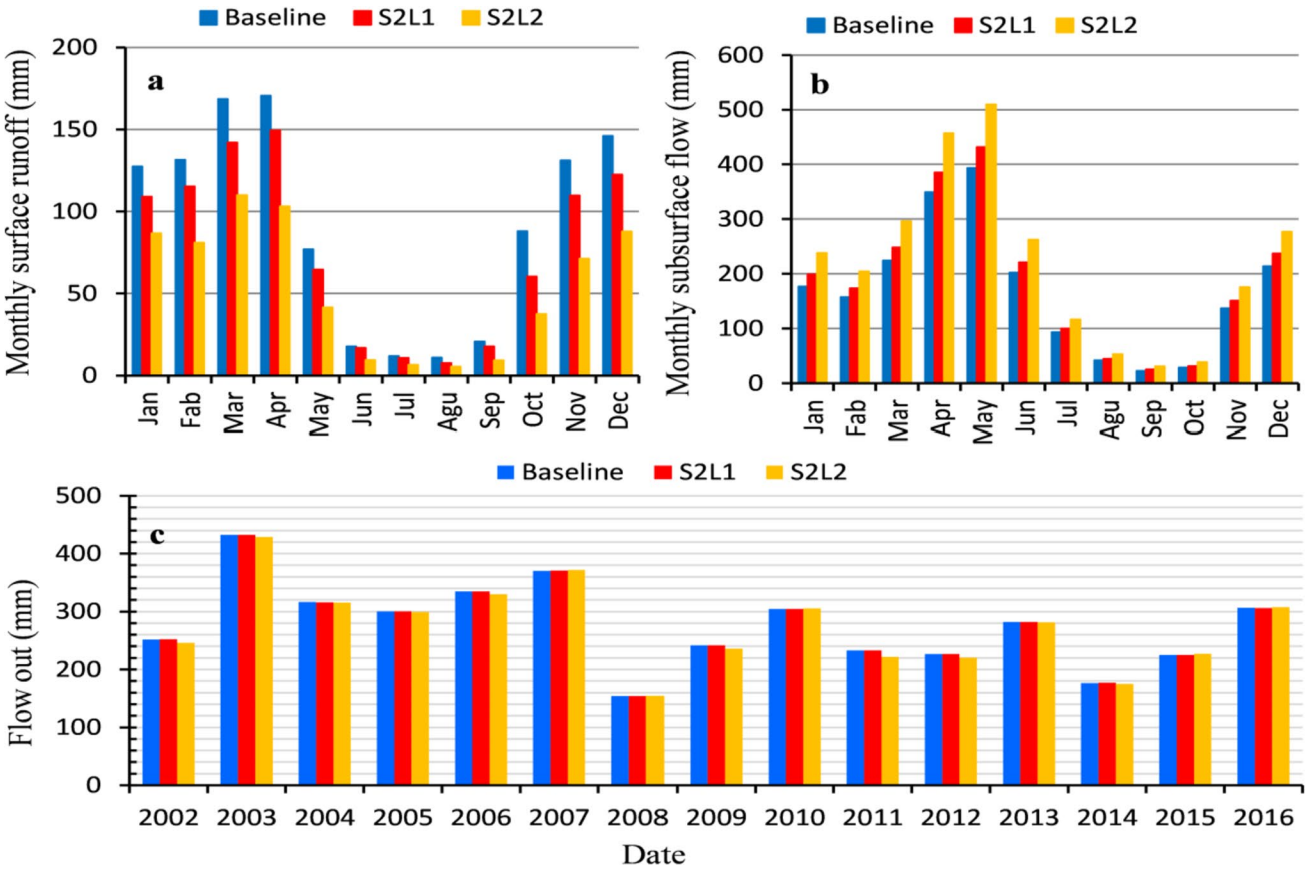

Fig. 7 The effects of the land-use scenarios (S2L1 and S2L2) on monthly surface runoff (**a**), monthly subsurface flow (**b**) and watershed flow out (**c**) compared to the baseline

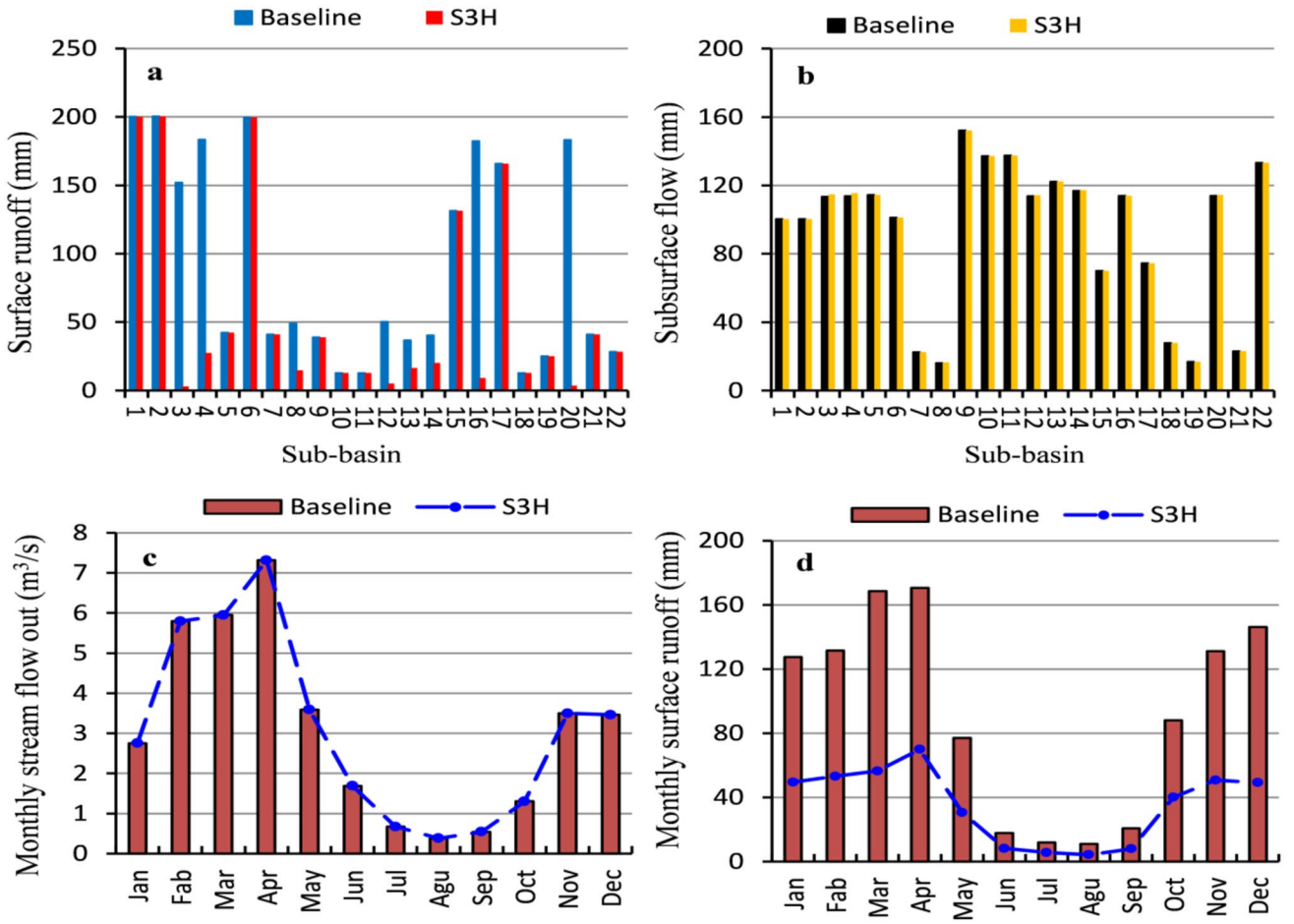

Fig. 8 The effect of hydraulic structures (scenario S3H) on the yearly average surface runoff in each sub-basin (**a**), yearly average subsurface flow in each sub-basin (**b**), monthly average stream flow out (**c**) and monthly average surface runoff (**d**)

more obvious in wet months, tending toward the least in dry months. However, this difference was not considerable.

Land-use scenarios

Executing the model with scenario S2L1 resulted in declining monthly surface runoff by an average of 16% in comparison with the baseline. In other words by restoring only 50% of the area of poor range land, the amount of surface runoff would reduce significantly. The percentage of declining in surface runoff was more considerable by applying S2L2, approximately 44%. (see Fig. 7a).

Surface runoff reduced more in months with high peak of discharge which highlights the impacts of vegetation density on increasing infiltration amount, reducing runoff and erosion damage.

Furthermore, the results of the land-use scenarios showed although they declined the amount of surface runoff, they increased the amount of subsurface flow instead (Fig. 7b). This means that watershed rehabilitation programs can be effective in storing water in soil without significant declining in water productivity of the watershed (see Fig. 7c). Moreover, it can increase the amount of base flow which contributes to the watershed flow out with a significant delay, especially in dry seasons.

Hydraulic structure scenario

Comparing the results of scenario S3H with the baseline showed that the yearly average surface runoff considerably decreased in the sub-basins which include hydraulic structures (Fig. 8a). Percentage of declining in the amount of surface runoff varied from 50 to 97%, depending on the volume of structures and type of the land use in each sub-basin. For instance, sub-basin #20 received the most decline in the amount of surface runoff which has the largest capacity of water storage. In contrast, it caused yearly average subsurface flow to increase slightly in those sub-basins (see Fig. 8b). For example, in sub-basin #4 amount of subsurface flow increased by 1.6 mm. It suggests that stored water in the

structures can infiltrate over the time and contribute to the subsurface flow. Furthermore, monthly stream flow out was not affected considerably, likewise land-use scenarios. This might be due to the mechanism of these structures which not store water permanently and their roles are mainly to make the concentration time of flow increase. Moreover, the percentage of changes in monthly surface runoff was 36% (Fig. 8d). It was larger than the change caused by S2L1, but smaller than S2L2. However, the structures have only been constructed in eight sub-basins. Generally, the results of this scenario showed that hydraulic structures played a dominant role with respect to controlling runoff in the watershed especially in flood season. These structures radically change water budget components, while declining runoff amount, supporting soil water storage, which in turn increase lateral and base flow amounts.

Conclusion

This study assessed the impacts of climate disturbance, land-use restoration and constructing hydraulic structures on hydrological components of a semiarid watershed using modeling approach. SWAT model was run and calibrated for an 18-year period with a four-year warm-up. Results of the model performance showed appropriate correspondence between observed and simulated monthly stream flow during calibration and validation periods. Results of the climate scenarios showed deficit in precipitation amount caused the monthly stream flow to decline, ranging from 37 to 15% for prolonging extreme drought and 34% to 12% for severe drought. The impact of land-use change was tested by two scenarios, including restoration of the area covered with RANGB to RANGE by 50% and 100% for scenarios S2L1 and S2L2, respectively. Results showed monthly surface runoff declined by 16% and 44% for S2L1 and S2L2, respectively. Constructing hydraulic structure scenario (S3H) resulted in a considerable decline in yearly runoff and a slight increase in subsurface flow. Furthermore, monthly surface runoff reduced more in flood season, but yearly stream flow out not significantly changed. Generally, present study showed that the most important driving force in changing stream flow was climate disturbance and although watershed management scenarios such as building check dams and pasture restoration reduced the amount of surface runoff, they caused water to infiltrate and supported subsurface flow. The results of this study provide a framework to analyze impacts of watershed management operations on hydrologic functioning of watersheds.

Acknowledgements This research was supported by a research fund of Soil Conservation and Watershed Management Research Institute (SCWMRI) of Iran. The authors are grateful for their logistic and funding supports. In addition, we would like to thank Dr. Jahangir Porhemmat for numerous interesting discussions on this topic.

Declarations The authors declare that there is no any conflict of interest in the subject matter or materials discussed in this manuscript.

References

Abbaspour KC (2011) SWAT-CUP4: SWAT calibration and uncertainty programs–a user manual. Swiss Federal Institute of Aquatic Science and Technology, Eawag 106

Anderson JR, Hardy EE, Roach JT, Witmer RE (1976) A land use and land cover classification system for use with remote sensor data. 964

Angela C-B, Javier C-J, Teresa G-M, Marisa M-H (2015) Hydrological evaluation of a Peri-urban stream and its impact on ecosystem services potential. Global Ecol Conserv 3:628–644

Arnold JG, Srinivasan R, Muttiah RS, Williams JR (1998) Large area hydrologic modeling and assessment part I: model develoment 1. J Am Water Resour Assoc 34:73–89

Bobadoye AO, Ogara WO, Ouma GO, Onono JO (2016) Assessing climate change adaptation strategies among rural Maasai pastoralist in Kenya. Am J Rural Dev 4:120–128

Sazeh-Ab-Shafagh Co (2016) Comperehensive—executive studies of aghasht watershed of Savojbolagh, Alborz Province.

Sabz-AndishPayesh Co (2018) Comperehensive: executive studies of Baraghan Watershed of Savojbolagh, Alborz Province

Fan M, Shibata H (2014) Spatial and temporal analysis of hydrological provision ecosystem services for watershed conservation planning of water resources. Water Resour Manage 28:3619–3636

Francesconi W, Srinivasan R, Pérez-Miñana E, Willcock SP, Quintero M (2016) Using the soil and water assessment tool (SWAT) to model ecosystem services: a systematic review. J Hydrol 535:625–636

Gao C, Booij MJ, Xu Y-P (2020) Impacts of climate change on characteristics of daily-scale rainfall events based on nine selected GCMs under four CMIP5 RCP scenarios in Qu River Basin, East China. Int J Climatol 40:887–907

Gathenya M, Mwangi H, Coe R, Sang J (2011) Climate- and land use-induced risks to watershed services in the Nyando River Basin, Kenya. Exp Agric 47:339–356

Ghoraba SM (2015) Hydrological modeling of the Simly Dam watershed (Pakistan) using GIS and SWAT model. Alex Eng J 54:583–594

Gupta HV, Sorooshian S, Yapo PO (1998) Toward improved calibration of hydrologic models: multiple and noncommensurable measures of information. Water Resour Res 34:751–763

Hargreaves GH, Samani ZA (1982) Estimating potential evapotranspiration. J Irrig Drain Div 108:225–230

Herrero M, Thornton PK, Kruska RL, Jones PG, Owiyo T, Kristjanson P, Notenbaert A, Bekele N, Omolo A (2006) Mapping climate vulnerability and poverty in Africa: report to the department for international development

Jain S, Tyagi J, Singh V (2010) Simulation of runoff and sediment yield for a Himalayan watershed using SWAT model. J Water Resour Prot 2010:267–281

Jung I, Bae D-H, Lee BJ (2013) Possible change in Korean streamflow seasonality based on multi-model climate projections. Hydrol Process 27:1033–1045

Karlsson IB et al (2016) Combined effects of climate models, hydrological model structures and land use scenarios on hydrological impacts of climate change. J Hydrol 535:301–317

Kim D-H, Jang T, Hwang S (2020) Evaluating impacts of climate change on hydrology and total nitrogen loads using coupled APEX-paddy and SWAT models. Paddy Water Environ, 18:515–529

Li E, Mu X, Zhao G, Gao P, Sun W (2016) Effects of check dams on runoff and sediment load in a semi-arid river basin of the Yellow River. Stoch Environ Res Risk Assess 31:1791–1803

Lin F, Chen X, Yao H, Lin F (2022) SWAT model-based quantification of the impact of land-use change on forest-regulated water flow. CATENA 211:105975

McKee TB, Doesken NJ, Kleist JR (1993) The relationship of drought frequency and duration to time scales

Moriasi ND, Arnold JG, Van Liew, MW, Bingner RL, Harmel RD, Veith TL (2007) Model evaluation guidelines for systematic quantification of accuracy in watershed simulations. Trans ASABE 50:885–900

Mukheibir P (2007) The impact of climate change on small municipal water resource management. The case of Bredasdorp, South Africa.

Nash JE, Sutcliffe JV (1970) River flow forecasting through conceptual models part I: a discussion of principles. J Hydrol 10:282–290

Ndulue EL, Ezenne GI, Mbajiorgu CC, Ogwo V, OgbuK N (2018) Hydrological modelling of upper Ebonyi watershed using the SWAT model. Int J Hydrol Sci Technol 8:120–133

Norman LM, Niraula R (2016) Model analysis of check dam impacts on long-term sediment and water budgets in Southeast Arizona, USA. Ecohydrol Hydrobiol 16:125–137

Osei MA, Amekudzi LK, Wemegah DD, Preko K, Gyawu ES, Obiri-Danso K (2019) The impact of climate and land-use changes on the hydrological processes of Owabi catchment from SWAT analysis. J Hydrol Reg Stud 25:100620

Piman T, Cochrane TA, Arias ME, Green A, Dat ND (2013) Assessment of flow changes from hydropower development and operations in Sekong, Sesan, and Srepok Rivers of the Mekong Basin. J Water Resour Plan Manag 139:723–732

Porhemmat J, Altafi Dadgar M (2023) Analysis of hydrological drought indices in Alpine Zagros Mountains of Iran. Arab J Geosci 16:594

Qasim M, Hubacek K, Termansen M (2013) Underlying and proximate driving causes of land use change in district Swat, Pakistan. Land Use Policy 34:146–157

Rodrigues DBB, Gupta HV, Mendiondo EM (2014) A blue/green water-based accounting framework for assessment of water security. Water Resour Res 50:7187–7205

Salmoral G, Willaarts BA, Troch PA, Garrido A (2015) Drivers influencing streamflow changes in the Upper Turia basin, Spain. Sci Total Environ 503–504:258–268

Sarmadian F, Rahimy P, Keshavarzi A (2010) Modeling of sediment yield and bicarbonate concentration in Kordan Watershed. J Agric Sci Technol 12:121–131

Shi P, Zhang Y, Ren Z, Yu Y, Li P, Gong J (2019) Land-use changes and check dams reducing runoff and sediment yield on the Loess Plateau of China. Sci Total Environ 664:984–994

Shukla S, Wood AW (2008) Use of a standardized runoff index for characterizing hydrologic drought. Geophys Res Lett 35

Tamm O, Maasikamäe S, Padari A, Tamm T (2018) Modelling the effects of land use and climate change on the water resources in the eastern Baltic Sea region using the SWAT model. CATENA 167:78–89

Wang Q, Liu R, Men C, Guo L, Miao Y (2018) Effects of dynamic land use inputs on improvement of SWAT model performance and uncertainty analysis of outputs. J Hydrol 563:874–886

Wu D, Cui Y, Xie X, Luo Y (2019) Improvement and testing of SWAT for multi-source irrigation systems with paddy rice. J Hydrol 568:1031–1041